Comparison of the crystal chemistry of selected MSi$_6$O$_{15}$-based silicates

S.M. HAILE[1] AND B.J. WUENSCH[2]

[1]Materials Science Department, California Institute of Technology, Pasadena, California 91125, U.S.A.
[2]Department of Materials Science and Engineering, Massachusetts Institute of Technology, Cambridge, Massachusetts 02139, U.S.A.

ABSTRACT

The structures of four A$_3$MSi$_6$O$_{15}$($\cdot n$H$_2$O) silicates (A = Na or K, M = Nd or Y) recently determined by the authors are compared with one another and with the structures of related silicates. The 2:5 Si:O ratio in these compounds (silicate tetrahedra linked by sharing three O atoms per tetrahedron plus one unshared O atom) permits layer, double-chain, or double-ring configurations. In α-K$_3$NdSi$_6$O$_{15}$·2H$_2$O, β-K$_3$NdSi$_6$O$_{15}$, and Na$_3$NdSi$_6$O$_{15}$·2H$_2$O, the linkage is found to result in a corrugated layered structure, in β-Na$_3$YSi$_6$O$_{15}$ a double-chain structure, and in α-Na$_3$YSi$_6$O$_{15}$ a unique double-ring structure. Although the factors that govern the stabilities of ring vs. chain vs. layered structures remain to be completely elucidated, it is apparent in the layered structures that larger M cations (such as Nd and Ce) produce a greater degree of corrugation than do Zr and Ti cations. The more open structures of neodymium and cerium silicates contain large channels that may serve as pathways for fast alkali ion transport.

INTRODUCTION

All physical models for description of the response of a material to applied forces require knowledge of the crystal structure as a critical starting point. Yet, prediction of structure, given a composition, is a goal that still eludes solid-state chemists and physicists for all but the simplest of metals and binary compounds. In a contribution toward understanding the crystal chemistry of silicate compounds, we compare the recently determined structures of four silicates synthesized by the authors: α-K$_3$NdSi$_6$O$_{15}$·2H$_2$O, β-K$_3$NdSi$_6$O$_{15}$, Na$_3$NdSi$_6$O$_{15}$·2H$_2$O, and α-Na$_3$YSi$_6$O$_{15}$. Because these compounds were synthesized under similar hydrothermal conditions, as described below, differences in structure are directly attributable to differences between the cation species involved and, hence, are examined in detail. We also compare these structures with some related A$_x$MSi$_6$O$_{15}$ compounds (A = alkali metal or alkaline earth metal and M = Y, Zr, or Ti). Together, these compounds constitute a subset of Si$_2$O$_5$-based silicates that do not form flat silicate layers. In subsequent discussion these phases are designated simply by the A and M cations present in the composition; the Si$_6$O$_{15}$ anion that they have in common will be omitted for brevity. The properties of these compounds are of interest because the MSi$_6$O$_{15}$ complex anions tend to crystallize with open frameworks, creating channels that may serve as pathways for fast alkali ion transport.

SYNTHESIS AND PHASE IDENTIFICATION

All of the compounds prepared by us were grown by hydrothermal methods, as described in detail elsewhere (Haile et al. 1993a, 1993b). In general, the products were obtained in the form of microcrystalline powders from isothermal experiments, in which the temperature was held typically at 500 °C and the pressure at 825 bar. The precursor material was usually a finely ground glass of composition A$_2$O-M$_2$O$_3$-17SiO$_2$. The solvent was either deionized water or a 0.1 M solution of the hydroxide or carbonate of the appropriate alkali cation. As customary in the hydrothermal technique, just enough solvent was added to platinum capsules to balance the pressure applied during crystallization. They were filled to a fraction that ranged from 0.3 to 0.7 depending on the exact synthesis conditions. Synthesis was carried out in a Tuttle autoclave in experiments that extended from 7 to 12 d.

The crystallization of Na$_3$Nd and α-Na$_3$Y (the latter is designated α to distinguish it from an isocompositional compound reported by Bourguiba and Dogguy 1994 and discussed below) was generally reproducible, but the stability range of both compounds in terms of pressure, temperature, and solution molarity was narrow. Consequently, they often appeared in conjunction with secondary phases. Slightly lower temperatures (350–500 °C) tended to produce Na$_3$Nd as a single phase, whereas slightly higher temperatures (500–600 °C) and pressures (1400 bar) tended to favor crystallization of α-Na$_3$Y as a single phase. A *Bb*2$_1$m form of K$_3$Nd (designated β) was obtained in only three experiments out of more than 100 that were conducted in the K$_2$O-Nd$_2$O$_3$-SiO$_2$ system, suggesting that it may be a metastable phase. The synthesis of a K$_3$Nd phase that was designated α was, in contrast, extremely reproducible and occurred over a wide range of synthesis conditions. It was possible to synthesize large crystals (0.1 × 2 × 1 mm³) in experiments that were

TABLE 1. Crystallographic data for the four alkali-rare earth silicates compared in the present work

Phase	Space group	a (Å)	b (Å)	c (Å)	Z
α-$K_3NdSi_6O_{15}\cdot2H_2O$	$Pbam$	16.008(2)	15.004(2)	7.2794(7)	4*
β-$K_3NdSi_6O_{15}$	$Bb2_1m$	14.370(2)	15.518(2)	14.265(2)	8†
$Na_3NdSi_6O_{15}\cdot2H_2O$	$Cmm2$	7.385(2)	30.831(7)	7.1168(13)	4‡
α-$Na_3YSi_6O_{15}$	$Ibmm$	10.468(2)	15.2467(13)	8.3855(6)	4§

* Haile and Wuensch, to be published. Isostructural to a phase reported earlier by Pushcharovskii et al. (1977).
† Haile and Wuensch, to be published.
‡ Haile et al. (1997). Related to a phase reported by Karpov et al. (1977).
§ Haile et al. (1995).

performed in a temperature gradient through use of a Morey autoclave (Haile et al. 1991).

The chemical compositions of the crystals so obtained were established with electron microprobe techniques. Data were collected with a JEOL Superprobe 733 equipped with a wavelength-dispersive detector. The intensities of the characteristic X-radiation peaks were converted to stoichiometric quantities using the ZAF data reduction procedure and appropriate standards. Where the microprobe measurements suggested the presence of H_2O in the structure, the H_2O content was also determined by thermogravimetric analysis combined with mass spectrometry of the emitted vapor. Crystal structures were determined by single-crystal X-ray techniques using diffraction data that were collected at room temperature in Mo$K\alpha$ radiation. Crystallographic data are provided in Table 1. Complete structure determinations, reported elsewhere (Haile et al. 1995, 1997; Haile and Wuensch, unpublished manuscript), confirmed the ideal compositions deduced from the microprobe and thermogravimetric analyses.

OVERVIEW OF STRUCTURES TO BE CONSIDERED

The main structural features of the four $A_3MSi_6O_{15}$-($\cdot nH_2O$) silicates synthesized in the present work are summarized in Table 2 along with similar data for four related silicates: β-$Na_3YSi_6O_{15}$ (Bourguiba and Dogguy 1994); dalyite, $K_2ZrSi_6O_{15}$ (Fleet 1965); armstrongite, $CaZrSi_6O_{15}$ (Kashaev and Sapozhnikov 1978); and $K_2CeSi_6O_{15}$ (Karpov et al. 1976). All of the structures are based on linkages of SiO_4 tetrahedra that share three of their four O corners with a corner of a neighboring SiO_4 group. The fourth vertex is unshared, being bonded to M (and, in some cases, A as well) rather than a second Si atom. This proportion of "bridging" to "terminating" O atoms accommodates the overall Si:O ratio of 2:5. In general, the Si-O_{term} bond distance is shorter than the Si-O_{br} distance, reflecting a stronger bond between Si and O than between the M (or A) cation and O.

A stoichiometry of $A_3MSi_6O_{15}$ provides six terminating O atoms per formula unit for each M cation. The ionic radius of the M cation, ~0.95 Å, suggests that this species is octahedrally coordinated by O ($r_O \approx 1.36$ Å). Thus, it is reasonable to expect that the six terminating O atoms available per M cation provide this coordination. In three of the compounds, α-K_3Nd, β-K_3Nd, and α-Na_3Y (and in

all four related compounds), octahedral coordination by terminating O atoms is indeed observed. In Na_3Nd, however, the Nd atom is sevenfold coordinated (one of its seven vertices consists of a bridging O atom), with the unusual consequence that it shares one of its polyhedral edges with that of an SiO_4 tetrahedron. As might be expected, the shared edge is shortened relative to other O-O distances in the structure, whereas the distances between the cations and the bridging O atoms are elongated. The increase in bond lengths results in a bond valence sum of 2.06 at the bridging O atom, which is only slightly greater than the average of 1.96(12) in the Na_3Nd structure (Haile et al. 1997).

From the data provided in Table 2 it is evident that (MSi_6O_{15})-based silicates readily adopt either single-layer structures in which isolated Si_2O_5 layers are linked only by bonds with A or M atoms or double-chain structures in which two chains are linked together by bridging O atoms. In addition to the single-layer and double-chain structures, Table 2 reveals that one compound, α-Na_3Y, adopts a double-ring structure and another, K_2Ce, adopts a three-dimensional framework structure. Possible reasons for the appearance of these rare, and presumably unfavorable, silicate anion configurations are discussed below, including a detailed comparison of K_2Ce with the single-layer silicates and α-Na_3Y individually.

DOUBLE-CHAIN SILICATES

Comparisons of the double-chain silicates have been made by others (see, for example, Ghose and Wan 1978) and we mention only briefly some key features that distinguish these from the single-layer silicates. First, the valences and sizes of the A and M cations appear to have little influence in determining which of these two general topologies is adopted: Both M^{3+} and M^{4+} cations appear in both types of structures, as do both A^+ and A^{2+}. The structural differences observed may, in fact, result from differences in synthesis conditions (layers tend to result from hydrothermal synthesis and chains from atmospheric, high-temperature crystallization), rather than differences in chemistry. It is also noteworthy that only one double-chain structure-type, that of zekterite, LiNaZr, has been observed. Epididymite, Na_2Be_2, and elpidite, Na_2Zr, can be considered distortions of the zekterite structure. In contrast, few of the single-layer compounds are isostructural to one another. Indeed, of seven single-layer

TABLE 2. Comparison of selected crystal-chemical parameters for the seven Si_6O_{15} phases examined in the present work

	α-K₃Nd	β-K₃Nd	Na₃Nd	α-Na₃Y	β-Na₃Y (b)	K₂Zr (c)	CaZr (e)	K₂Ce (f)
Structure	single layer	single layer	single layer	double ring	double chain	single layer	single layer	framework
Known isomorphs	—	HNa₂Ce* (a)	—	—	many†	K₂Ti (d)	—	—
Vol/p.f.u. (Å³)	437.1(1)	397.6(1)	405.1(1)	334.6(1)	348.9(1)	334.8	365.9	336.6
⟨Si-O$_t$⟩ (Å)	1.579(7)	1.575(9)	1.581(9)	1.576(9)	1.588(4)	1.616(13)	1.61	1.598(6)
⟨Si-O$_{br}$⟩ (Å)	1.628(7)	1.633(10)	1.628(8)	1.641(2)	1.637(4)	1.625(13)	1.63	1.626(10)
⟨O-O⟩ (Å)	2.635(12)	2.640(14)	2.636(11)	2.651(3)	2.654	2.65(2)	2.65	2.639
⟨Si-O-Si⟩ (°)	144.1(5)	139.3(9)	142.4(6)	133.3(2)	150.2	146.9	151	141.9
M cation	Nd³⁺	Nd³⁺	Nd³⁺	Y³⁺	Y³⁺	Zr⁴⁺	Zr⁴⁺	Ce⁴⁺
Coordination	6	6	7	6	6	6	6	6
Ionic radius (Å)	0.983	0.983	0.99	0.90	0.90	0.72	0.72	0.80
⟨M-O⟩ (Å)	2.359(7)	2.373(9)	2.437(9)	2.250(2)	2.244(4)	2.064(12)	2.09	2.228(3)
⟨O-O⟩ (Å)	3.333(11)	3.359(14)	3.156(11)	3.180(5)	3.177	2.92	2.91	3.203
Electroneg.	1.14	1.14	1.14	1.22	1.22	1.33	1.33	1.12
A cation	K	K	Na	Na	Na	K₀.₈₅Na₀.₁₅	Ca	K
Coordination‡	6, 7	5, 6	4, 5	5, 6	8, 9, 10	8	4	8
Ionic radius (Å)	1.38, 1.46	1.38	0.99, 1.00	1.00, 1.02	1.16, 1.32	~1.46	1.00	1.51
Electroneg.	0.82	0.82	0.93	0.93	0.93	~0.84	1.00	0.82
R_F	0.053	0.042	0.026	0.036	0.048	0.108	0.13	0.022

Notes: Number in parentheses after an average value reflects the maximum standard deviation reported for any individual value as determined from the diffraction data refinement. It does not reflect the spread in individual values used to calculate the average. Sources: (a) Shumyatskaya et al. (1980); (b) Bourguiba and Dogguy (1994); (c) Fleet (1965); (d) Gerbert et al. (1983); Lazebnik et al. (1984); (e) Kashaev and Sapozhnikov (1978); (f) Karpov et al. (1976).

* The MSi_6O_{15} framework is virtually identical to that of β-K₃Nd, however, the arrangement of alkali ions differs.

† Known isomorphs include Na₂LiYSi₆O₁₅ (Gunawardane et al. 1982); NaLiZrSi₆O₁₅ = zekterite (Ghose and Wan 1978); NaLiTiSi₆O₁₅, LiNaSnSi₆O₁₅ (Marr and Glasser 1979); Na₂LiFeSi₆O₁₅ = emeleusite (Johnson et al. 1978); Li₂ZrSi₆O₁₅ (Quintana and West 1981); (Na,K)Fe²⁺Fe³⁺Si₆O₁₅·0.5H₂O = tuhualite (Merlino 1969); and Na₂Mg₂Si₆O₁₅ (Cradwick and Taylor 1972). Related structures include Na₂ZrSi₆O₁₅·3H₂O = elpidite (Cannillo et al. 1973); Na₂Be₂Si₆O₁₅·H₂O = epididymite—here two edge-sharing BeO₄ groups play the role of a single MO₆ group (Robinson and Fang 1970).

‡ Defined as the number of O neighbors less than 3.3 Å away or as authors have reported. In the case of Na and Ca, where the ions appear fourfold coordinated, neighboring H₂O molecules, in fact, provide for sixfold coordination.

MSi_6O_{15} structures that have been reported only two pairs of isomorphs occur. The zekterite structure-type contains two large A cation sites (eight- to tenfold coordinated), one small A cation site (fourfold coordinated), and one M cation site (sixfold coordinated). These features provide a capacity for accommodation of cations of varying size and valence, attributed by Gunawardane et al. (1982) as the result of the unique ability of this structure to balance local distortions at the tetrahedral (A) and octahedral (M) sites in a manner that minimizes distortions of the silicate chain. Bourguiba and Dogguy (1994) suggested that the chain itself is quite flexible. In the case of β-Na₃Y, the distortions at the usually tetrahedral site are so great as to cause the coordination at this site to become eightfold.

LAYERED STRUCTURES

The connectivity of tetrahedra in the silicate sheets

The single-layer structures of α-K₃Nd, β-K₃Nd, Na₃Nd, dalyite, and armstrongite have in common a wollastonite-type chain (Ohashi and Finger 1978), as the basic structural building block (Fig. 1a). In the terminology of Liebau (1985), this is a dreier-single chain, meaning that the translational repeat unit along the chain consists of three silicate tetrahedra and that the tetrahedra are linked only to others that extend along the direction of the chain. Viewed along the direction of the chain, the wollastonite-type chain has a width of two silicate tetrahedra. Condensation of two wollastonite-type chains produces the xonotlite-like chain (Kudoh and Takéuchi 1979), a dreier-double chain, shown in Figure 1b. This chain is

characterized by the presence of eight-membered silicate rings. Further condensation of xonotlite-like chains produces the connectivity of tetrahedra in the sheets found within all of the single-layer A₃MSi₆O₁₅(·nH₂O) structures under present consideration. Condensation of the xonotlite-like chains in a direction normal to the chain results in the formation of alternating four- and six-membered rings at the interface between them, (Fig. 1c). Alternatively, the position of the xonotlite-like chains can be sheared by one-half of the chain repeat distance prior to condensation. A sequence of five-membered rings then occurs along the interface (Fig. 1d), once the sheet is distorted to permit rejoining the bridging O atoms.

The layers revealed by the structure determinations are shown schematically in Figure 2. Severe corrugation of the layers was neglected in this representation. Unshaded tetrahedra indicate polyhedra for which the terminating or apical O atom is above the plane of the sheet (an "upward directed" tetrahedron), whereas shading indicates that the O atom resides below the plane ("downward directed"). In the two K₃Nd silicate structures (Figs. 2a and 2b) and in armstrongite, CaZr, (Fig. 2d) the xonotlite-like chains condense in a direction normal to the chain as in Figure 1c. Disregarding the directedness of the tetrahedra, neighboring xonotlite-like chains are directly related by translation, and, for this idealized case, the periodicity perpendicular to the chains is equal to the width of four silicate tetrahedra (i.e., the width of the xonotlite-like chain). The same is true in dalyite, K₂Zr (Fig. 2e), although in this structure the layer is significantly distorted from the idealized rectangular nets that are characteristic
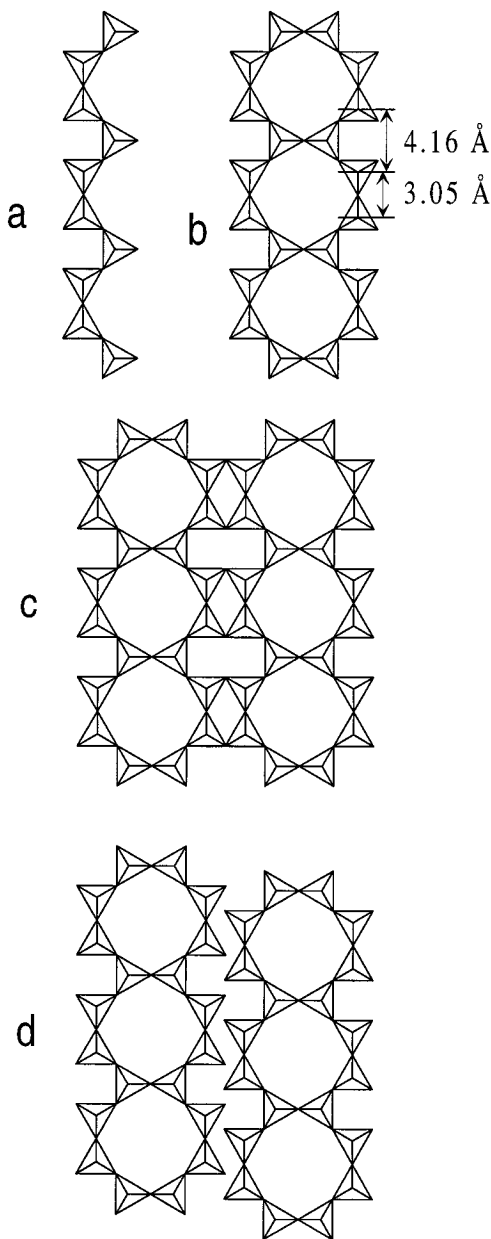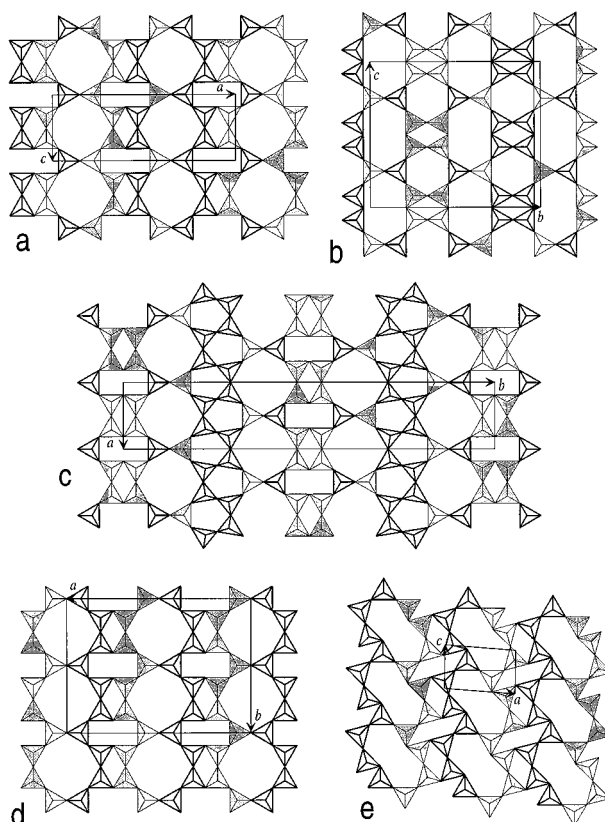
FIGURE 1. Idealized representations of building blocks for layered silicates. (**a**) The wollastonite-type chain and its three-tetrahedron repetition. (**b**) Condensation of two wollastonite-type chains to form the xonotlite-like double chain with a characteristic eight-membered ring. The distances shown between unshared apical vertices of the tetrahedra assume no distortion of the idealized chain and an Si-O distance of 1.62 Å. (**c**) Condensation of a pair of xonotlite-like chains to form a portion of the Si$_2$O$_5$ layer found in α- and β-K$_3$Nd silicate. Four-membered and six-membered rings alternate along the interface of the xonotlite-like units. (**d**) Condensation of a pair of xonotlite-like chains after a shear equal to one-half of the periodicity of the chain. Closure of the corners of tetrahedra across the interface by distortion of the chains results in a sequence of five-membered rings along the interface as in the Si$_2$O$_5$ layer found in Na$_3$Nd silicate.

of the first three structures. The silicate sheets of Na$_3$Nd (Fig. 2c) are somewhat more complex. Pairs of xonotlite-like chains again come together to form six- and four-membered rings at their interface as in the K$_3$Nd phases, but alternate chains condense with shear so that five-membered rings are generated at the second interface as in Figure 1d. Repetition of these alternating modes of condensation produces a total offset equal to the chain periodicity and thus leads to centering of the face of the unit cell that is parallel to the layer. It is noteworthy that in the zirconium silicates armstrongite and dalyite, all tetrahedra along each wollastonite-type chain are pointed in the same direction, whereas in the neodymium silicates, the directedness alternates along the chain.
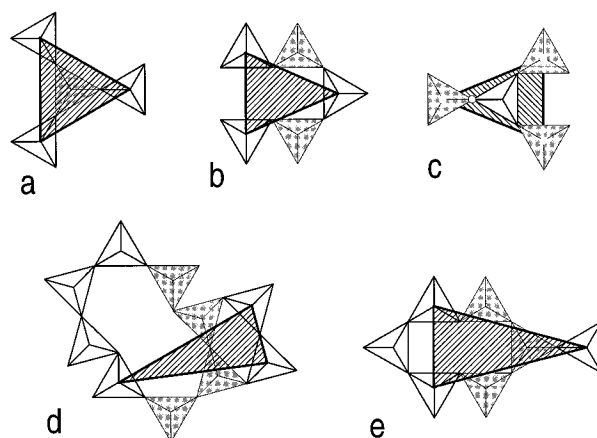
The coordination polyhedra around the rare-earth cation, M, link neighboring silicate sheets to form a three-dimensional framework. In all but the sodium neodymium silicate, octahedra around these cations derive three of their O neighbors (i.e., one face) from a layer below and the remaining three (i.e., the opposite face) from a layer above the cation. Hence, the location and geometry of the M polyhedra are intimately tied to the directedness of silicate tetrahedra. Returning to the basic structural unit, the wollastonite-type chain, there are two apical O-O distances that are comparable to the lengths of typical edges in M polyhedra (Belov 1961). In the idealized geometry shown in Figure 2b, the distance between the apical O atoms of two neighboring SiO$_4$ tetrahedra with the same directedness is 3.05 Å; that between the apical O atoms of two tetrahedra separated by a third in different orientation is 4.16 Å. Again, it is assumed that the tetrahedra are pointed in the same direction. The former distance is essentially fixed by the geometry of the SiO$_4$ tetrahedra and the Si-O-Si angle. The latter distance, however, can vary because the two tetrahedra providing the coordinating, apical O atoms have no fixed relationship to one another. To complete a triangular face of the octahedron, a third O neighbor is needed. This derives from either a neighboring wollastonite-type chain or from a chain further removed. To bring this O atom to a reasonable distance from the M cation, all of the layers, shown in idealized form in Figure 2, become highly corrugated in the actual structures along the direction perpendicular to the wollastonite-type chains. In general, there is little corrugation along the length of the chains.

The positioning of the octahedral faces of the M polyhedron relative to the apical terminal O ions in the silicate layers of Figure 2 is depicted in Figure 3. The triangular faces in the neodymium silicates contain O atoms from neighboring wollastonite-type chains in accord with the distribution of upward- and downward-directed tetrahedra. This is true also of Na$_3$Nd (Fig. 3c) but, as a consequence of the sevenfold coordination of Nd, a fourth bond to a bridging O is present within the triangle. The tetrahedra in neighboring chains all point in the opposite direction in the zirconium silicates. The triangular faces therefore join apical O atoms from every second chain (Figs. 3d and 3e). Consequently, the manner in

FIGURE 2. Idealized representation of the connectivity of the silicate tetrahedra in the Si$_6$O$_{15}$ layers found in (**a**) α-K$_3$Nd, (**b**) β-K$_3$Nd, (**c**) Na$_3$Nd, (**d**) CaZr, and (**e**) K$_2$Zr. Unshaded tetrahedra indicate polyhedra for which the terminating or apical O atom is above the plane of the sheet (an "upward directed" tetrahedron), whereas shading indicates that the O resides below the plane ("downward directed"). The actual configurations of these sheets display pronounced hills and valleys that run parallel to the wollastonite-type chains.

FIGURE 3. Linkage of the apical vertices of the tetrahedra in the Si$_6$O$_{15}$ layers by a triangular face of an MO$_x$ polyhedron. The vertices of the shaded tetrahedra point downward and do not participate in the linkage. (**a**) α-K$_3$Nd, β-K$_3$Nd, and Na$_3$Nd; (**b**) α-K$_3$Nd; (**c**) in Na$_3$Nd the four O atoms that form bonds to the sevenfold-coordinated Nd are represented by small circles and include one bridging O atom. (**d**) dalyite, K$_2$Zr; (**e**) armstrongite, CaZr. Note that the silicate tetrahedra are depicted in an idealized, undistorted, planar arrangement. Marked corrugation of the layers parallel to the direction of the wollastonite-type chains in the actual structures reduces the separation of the vertices along the horizontal direction of the diagram. This results in a much more equilateral shape for the face of the MO$_x$ polyhedron.

which the silicate layers are corrugated and the way in which neighboring layers are related in the Zr silicates are very different from that in the neodymium silicates. As can be seen in Figure 4, which provides idealized projections of the structures along the direction of the wollastonite-type chains, the corrugations are such that a neodymium polyhedron spans three silicate tetrahedra (in a direction normal to the wollastonite-type chain), whereas in the zirconium silicates the Zr octahedra span four. The degree of warping of the layers is therefore greater in the former than in the latter. Moreover, the layers in the zirconium silicates are stacked in a staggered, two-layer sequence that gives rise to a centered unit cell. In contrast, neighboring layers in the neodymium silicates are stacked essentially by translation normal to the layers. The structure of α-K$_3$Nd is, however, somewhat more complicated than that of the other two neodymium silicates. The α-phase has a two-layer stacking sequence in which neighboring layers are related by a twofold rotation axis parallel to the corrugations, rather than by transla-

tion. The basic geometric features represented in Figure 4 remain present, however.

In both the neodymium and the zirconium silicates, the overall stoichiometry requires that there should be two MO$_6$ octahedra for every eight silicate tetrahedra along the direction of the corrugation. Hence, in the neodymium silicates a large channel is formed by the "non-participation" of two out of eight silicate tetrahedra (at least on one side of a given layer) in the formation of MO$_6$ octahedra (Fig. 4a). In the zirconium silicates, by contrast, no such channels are formed. Indeed, the small channels suggested for the zirconium silicates by Figure 4b are not really present in the true structures because of distortions from the idealized arrangement that is depicted. The greater openness of the neodymia-silicate frameworks over those of the zirconia silicates is evidenced by the significantly greater volumes per formula unit in the neodymium silicate structures (Table 2).

At first glance, it is somewhat counterintuitive that bonding across four tetrahedra (Fig. 4b) should be necessary to provide more favorable conformation with the shorter O-O distances of the ZrO$_6$ octahedra instead of bonding across three (Fig. 4a). However, bringing the O atoms closer together in the latter configuration would force the Si-O-Si angles to adopt small and energetically unfavorable values. That the neodymia-silicate framework is preferred by larger M cations is evidenced by the structure of sazhinite, HNa$_2$CeSi$_6$O$_{15}$ (Shumyatskaya et al. 1980). This compound is formed with a Ce^{3+} ion that has

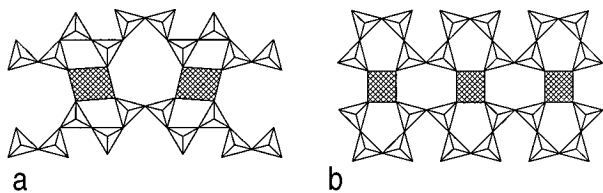**FIGURE 4.** The MSi_6O_{15} framework formed upon linkage of silicate layers by MO_x polyhedra: (**a**) neodymium silicates; (**b**) zirconium silicates.

a radius of 1.01 Å and displays a $CeSi_6O_{15}$ framework that is virtually identical to the $NdSi_6O_{15}$ framework of β-$K_3NdSi_6O_{15}$.

It is noteworthy that a silicate layer of the type observed in these MSi_6O_{15} silicates is also found in $K_2Be_2Si_6O_{15}$ (Nuamova et al. 1976), a compound that, strictly speaking, has no octahedrally coordinated M cation. The distribution of four-, six- and eight-membered rings and the directedness of silicate tetrahedra are identical to that in α-K_3Nd. Two Be atoms are tetrahedrally coordinated and share an edge in such a way that six O atoms effectively form a distorted octahedron about each pair of Be atoms. As in the case of the MSi_6O_{15} silicates, the six O atoms that form this octahedron are all terminating atoms with respect to the linkage of silicate tetrahedra. The Be_2O_6 pseudo-octahedron is, however, much smaller than the octahedra around the M cations in the silicates described above. The average Be-O distance is 1.644 Å and the average length of an O-O edge of the polyhedron 2.678 Å. As might be expected on the basis of these local geometric differences, the manner in which the Be_2O_6 pseudo-octahedra are linked to the Si_2O_5 layers differs significantly from that of the MO_x polyhedra. Four of the six O atoms in Be_2O_6 derive from a layer below the Be atoms and two derive from a layer above. Consequently, two of the faces of the pseudo-octahedron are formed by O atoms within the same silicate layer (Fig. 5a). One of these faces is equivalent to that found in α-K_3Nd, β-K_3Nd, and Na_3Nd (Fig. 3a) and the other to the octahedral face present in CaZr (Fig. 3e). The Be_2O_6 group thus spans four neighboring wollastonite chains and introduces an even higher degree of corrugation in the Si_2O_5 layer than do the ZrO_6 octahedra in CaZr and K_2Zr. Neighboring silicate layers in K_2Be_2 are related by translation, and the remaining two O atoms of the pseudo-octahedron derive from downward-directed silicate tetrahedra that are translationally equivalent to two of those of Figure 5a. Specifically, the apices of two shaded tetrahedra that are vertically displaced from one another provide the remainder of the coordination. The two shaded tetrahedra that are horizontally displaced from one another form part of other Be_2O_6 groups. The $Be_2Si_6O_{15}$ framework of K_2Be_2 is shown in Figure 5b. The much greater extent of layer warping in this structure in comparison with the MSi_6O_{15} structures (Fig. 4) is clearly evident.

Origin of the corrugations

On the basis of the six single-layer silicate structures that have been compared we conclude that as the octahedrally coordinated M cation decreases in size from Nd^{3+} to Zr^{4+} to $(Be_2)^{4+}$ the degree of corrugation of the layers increases commensurably. This occurs because a high degree of corrugation permits terminating O atoms to come within sufficient proximity to one another to satisfy the coordination requirements of a small M cation.

Liebau (1985) has conducted a broad analysis of the impact of A and M cation species on silicate layer topology. His first observation, that for a fixed average valence smaller cations tend to induce greater degrees of layer warping, is entirely in agreement with the results presented here. Liebau's second observation concerns the impact of A and M cation valence on layer topology. He noted that as the average valence of the A and M cations increases and, accordingly, the number of cations per silicate tetrahedra decreases, the compatibility of those cations with flat silicate layers decreases. Hence, the degree of layer warping increases. This second conclusion is only partially borne out by the silicates examined in the present work. The K_3Nd, Na_3Nd, and α-Na_3Y compounds have a lower average cation valence (0.67) and greater number of cations per six SiO_4 tetrahedra (4) than do the K_2Zr and CaZr compounds and indeed exhibit less corrugation in their layers than the latter. However, K_2Be_2 has the same average cation valence and number of cations per silicate tetrahedron as the neodymium silicates, yet has the most highly corrugated layers of the three types of single-layer silicates examined. Furthermore, one would expect K_2Zr and CaZr to have very different degrees of layer corrugation if one employed valence arguments alone, yet the corrugation in the respective layers is similar.

The framework structure of K_2Ce

The related compound K_2Ce takes on an "interrupted framework" structure rather than a single-layer motif, (Table 2). Karpov et al. (1976) identified xonotlite-like chains as the basic structural unit of this structure. The structure can also be understood in terms of (Si_5O_{13}) layers, containing six- and ten-membered silicate rings, that are linked together by bridging O atoms to form the three-dimensional silicate anion (Fig. 6). Although the positioning of the octahedral faces of the Ce polyhedron relative to the terminal O atoms cannot be described in terms of the geometries of Figure 3 (such groupings of silicate tetrahedra do not exist in K_2Ce), it is noteworthy that, as with the other MSi_6O_{15} structures, three of the O atoms derive from a layer above the Ce atom and three from a layer below. The extreme elongation of the ten-membered rings leads to a structure in which terminating O atoms are within close enough proximity to form the face of a CeO_6 octahedron without significant corrugation of the layers. Moreover, as with K_2Zr (and unlike the other MSi_6O_{15} compounds) two of the O-O edges in the
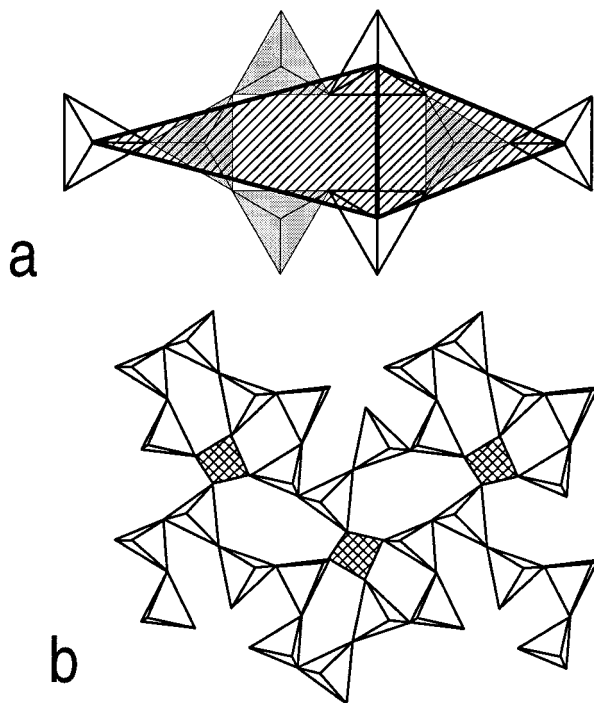
FIGURE 5. Structural features of K$_2$Be$_2$Si$_6$O$_{15}$ (Nuamova et al. 1976): (**a**) Linkage of the apical vertices of the tetrahedra in the Si$_6$O$_{15}$ layers by two triangular faces of a Be$_2$O$_6$ group. The vertices of the shaded tetrahedra point downward and do not participate in the linkage. (**b**) The Be$_2$Si$_6$O$_{15}$ framework.

FIGURE 6. Projection of an Si$_5$O$_{13}$ layer present in the framework silicate K$_2$CeSi$_6$O$_{15}$ (Karpov et al. 1976), along a direction normal to (100). Unshaded tetrahedra are upward directed, whereas those that are shaded are downward directed. Arrows indicate the locations of the bridging O atoms at which the layer is linked to others (not shown) to form a three-dimensional structure. Hatched triangles correspond to the faces of two distinct CeO$_6$ octahedra, one above the plane of the layer and one below.

octahedron are formed by terminating O atoms that derive from neighboring (i.e., directly linked) silicate tetrahedra. As discussed above, such a configuration provides a relatively short O-O distance and more readily accommodates the slightly smaller M cations in these structures.

The adoption of a framework structure by K$_2$Ce has been explained by Liebau in terms of a combined valence-cation size argument. He suggested that the high degree of layer warping that would be induced by the high average valence (low number of A and M cations per silicate tetrahedra) would result in the creation of interstitial sites between silicate layers that are too small for the Ce^{4+} cation (sixfold coordination for an ion of 0.80 Å radius). Stated alternatively, although the large Ce^{4+} cation may be stable in a layer structure with a relatively low degree of corrugation, the high valence is compatible only with a high degree of corrugation, and thus no layer can accommodate both the valence and the size requirements. Although this may be true, it is also quite possible that the absence of a single-layer structure for K$_2$Ce results from synthesis conditions that favored the observed framework structure. Indeed, in light of the similarity of the layers in K$_2$Zr and CaZr and the differences between the layers of the A$_3$Nd phases and K$_2$Be$_2$, it appears that size, not valence, determines the degree of layer corrugation. Therefore, under appropriate synthesis conditions it might be expected that the compound K$_2$Ce

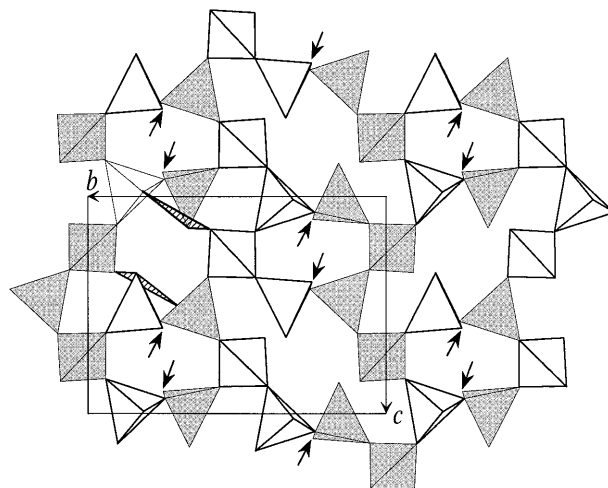could adopt a single-layer structure in which the corrugation is similar to that in the A$_3$Nd structures, because these contain an octahedral site sufficiently large for the Ce^{4+} cation.

This prediction is, to some extent, supported by the existence of corrugated layers in sazhinite, a cerium silicate isostructural to β-K$_3$Nd (Table 2). At first glance, the structural differences observed between the two cerium silicates are explained readily by the differences in stoichiometry and valence of the A and M cations: HNa$_2$Ce^{3+} vs. K$_2$Ce. However, for neither structure determination was the assigned stoichiometry or valence confirmed by a chemical analysis. Indeed, in an earlier work, the chemical formula of sazhinite was reported as Na$_3$Ce^{3+}Si$_6$O$_{15}$·6H$_2$O (Es'kova et al. 1974). Furthermore, the assignment of an OH group to one of the terminating O sites in the later refinement is not justified in terms of the Si-O(H) and Ce-O(H) bond lengths. Normally, metal-hydroxyl group bonds are longer than metal-oxygen bonds, but no unusually long bonds are present in the model refined by Shumyatskaya et al. (1979). Thus, it is quite possible that the actual stoichiometry of this mineral is Na$_2$Ce^{4+}Si$_6$O$_{15}$·nH$_2$O. In such case, sazhinite would then provide an example of Ce^{4+} existing in a single-layer silicate.

THE ISOLATED Si$_6$O$_{15}$ UNIT

The structure determined for α-Na$_3$YSi$_6$O$_{15}$ (Haile et al. 1995) contains an unusual, discrete Si$_6$O$_{15}$ unit that is shown in Figure 7a. It is, in the terminology of Liebau, a dreier-double ring, indicating that it is composed of two three-membered rings that share a common interfacial
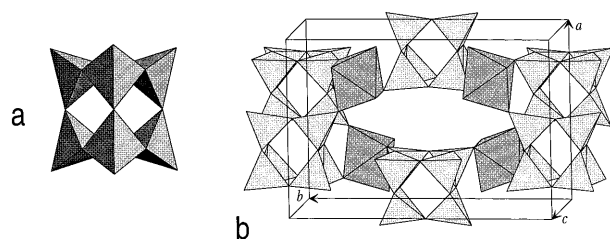
FIGURE 7. The structure determined for Na$_3$YSi$_6$O$_{15}$: (**a**) The unique isolated Si$_6$O$_{15}$ unit in the form of a dreier-double ring. (**b**) The YSi$_6$O$_{15}$ framework.

FIGURE 8. The average distance between Si and the bridging O atoms found in the Si tetrahedra of the present A$_3$MSi$_6$O$_{15}$·(nH$_2$O) silicates correlated with the secant of the Si-O-Si angle. The vertical bars indicate the maximum standard deviation that was present in any distance that was used in the average for each structure. The straight line is a linear-regression fit to data in the literature as determined by Hill and Gibbs (1979).

plane. The rarity of this unit results from the small Si-O-Si angles to which it gives rise. This may be seen from the data provided in Table 2. Indeed the Si-O-Si angle in α-Na$_3$Y is substantially smaller in comparison with β-Na$_3$Y. To accommodate this small angle, as is apparent from Table 2, the Si-O$_{br}$ bond distances are elongated relative to the other structures investigated. Hill and Gibbs (1979) have examined the relationship between Si-O-Si angle and Si-O$_{br}$ distance and concluded that the latter is linearly related to the secant of the angle. In Figure 8, we compare the average values obtained in our four silicates with the results of the linear regression analysis of Hill and Gibbs. It is evident that the data for our structures agree well with the relationship.

The Si$_6$O$_{15}$ units in α-Na$_3$Y are linked by YO$_6$ octahedra to form a three-dimensional network (Fig. 7b). In this case, unlike that of the layered silicates, the octahedron is essentially free to take on the most favorable configuration without the need to conform to O-O distances in the silicate anion. This configuration, combined with the compactness of the dreier-double ring, turns out to provide a structure with a much denser arrangement than in the layered silicates, as evidenced by the much smaller volume per formula unit. The high density explains why higher pressures facilitated more ready synthesis of the α-Na$_3$Y phase.

The higher density of α-Na$_3$Y relative to that of the β form suggests that the nature of the conditions of synthesis may account for these strikingly different polymorphic forms. The dreier-double ring structure was formed from hydrothermal solutions at 500–600 °C and 1400 bar, the highest pressures used in our syntheses. In contrast, β-Na$_3$Y was produced at 850 °C and ambient pressure by crystallization from a flux of Na$_2$MoO$_4$ and P$_2$O$_5$. In addition, β-Na$_3$Y contains the M^{3+} ion of largest radius known to result in formation of the zekterite structure-type and thus may be at the limit of structural stability for this configuration. The large Si-O-Si angles that occur in the chain imply that strain is necessary to match the Si$_6$O$_{15}$ to a cation as large as Y^{3+}. The existence of two polymorphs of Na$_3$Y demonstrates that it can be misleading to attribute differences in structure solely to differences in chemistry when different synthesis conditions are used or when synthesis conditions are unknown.
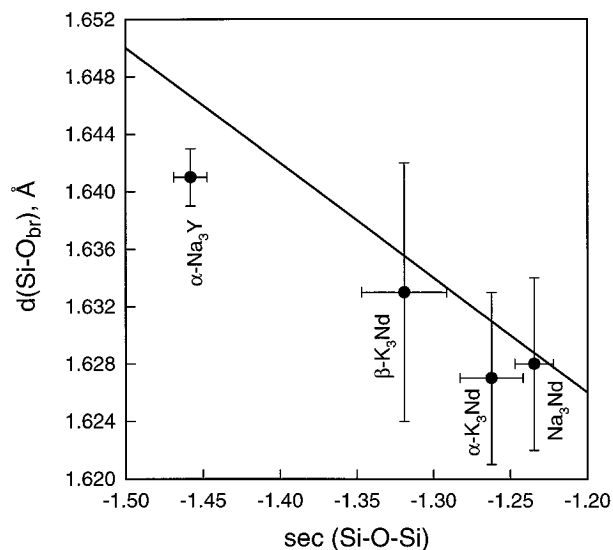
The reasons for the gross differences between the

α-Na$_3$Y structure and those displayed by the three other A$_3$MSi$_6$O$_{15}$ silicates examined in this work are not immediately apparent. We earlier suggested (Haile et al. 1995) that the greater electronegativity of Y relative to Nd resulted in an effectively smaller charge per silicate tetrahedron, permitting the silicate groups to come within closer proximity to each other. Alternatively (or perhaps additionally), it is possible that a layered yttrium silicate was not obtained because YO$_6$ cannot match either of the general motifs shown for the corrugated layers of Figure 4. The Y octahedron is perhaps too small for the neodymium configuration and too large for the zirconium model. However, given the many isomorphic zirconium and yttrium silicates (for example, the double-chain silicates listed in Table 2), it would be surprising if yttrium could not fit into the dalyite or armstrongite structure types. Indeed, any explanation based on size alone is somewhat unsatisfying. It is hard to imagine, given the myriad connectivities and modes of distortion with which an Si$_6$O$_{15}$ layer might be designed, that not a single one could conform to the geometry of the YO$_6$ octahedron.

Moreover, although the isolated dreier-double ring was observed only in the Na$_2$O-Y$_2$O$_3$-SiO$_2$ system, it may be premature to conclude that no layered silicate structures exist in this system. The structures of all compounds that we encountered in the sodium and potassium Nd$_2$O$_3$-SiO$_2$ systems have either been solved or found to possess previously known structure types. However several crystalline phases with structures that are as yet unsolved were reproducibly obtained in the Na$_2$O-Y$_2$O$_3$-SiO$_2$ system (Haile et al. 1993a). Several unique phases were identi-

fied on the basis of their powder diffraction patterns, but poor crystal quality precluded structure determinations. It is quite likely that some of these may be layered silicates.

CONCLUSIONS

The variety of silicate structures observed for these compositionally similar materials suggests that the energy differences between the various configurations are quite small. The reasons why a structure with the unique dreier-double ring was assumed by the phase with composition $Na_3YSi_6O_{15}$ remain to be completely explained. In contrast to yttrium silicate, both neodymium and zirconium silicates readily crystallize as layered structures, despite the significant differences between these ions in terms of charge and size. The Si_6O_{15} sheets in these structures assume highly corrugated configurations to conform to the geometry of the MO_6 (or MO_7) polyhedron. The differences in size between NdO_6 (or NdO_7) and ZrO_6 produce differences in the manner in which corrugation occurs, generating much more open structures in the case of the neodymium (and cerium) silicates than obtained in zirconium (and titanium) silicates. This openness results in large channels within the structures and suggests that layered neodymium and cerium silicates are, in general, more likely candidates for phases that may exhibit high ionic conductivity.

ACKNOWLEDGMENTS

REFERENCES CITED

Belov, N.V. (1961) Crystal chemistry of large cation silicates, p. 13–26. Consultants Bureau, New York.

Bourguiba, N.F. and Dogguy, L.S. (1994) Preparation et affinement de la structure d'un silicate a double chaines d'yttrium et de trisodium. Materials Research Bulletin, 29, 427–436.

Cannillo, E., Rossi, G., and Ungaretti, L. (1973) The crystal structure of elpidite. American Mineralogist, 58, 106–109.

Cradwick, M.E. and Taylor, H.F.W. (1972) The crystal structure of $Na_2Mg_2Si_6O_{15}$. Acta Crystallographica, B28, 3583–3587.

Es'kova, E.M., Semenov, E.I., Khomyakov, A.P., Kazakova, M.E., and Shumyatskaya, N.G. (1974). Zapiski Vsesoyuznogo Mineralogicheskogo Obshchestva, 103, 338–341. (Quoted in Soviet Physics Crystallography, 25, 419–423).

Fleet, S.G. (1965) The crystal structure of dalyite. Zeitschrift für Kristallographie, 121, 349–368.

Gerbert, W., Medenbach, O., and Flörke, O.W. (1983) Darstellung und Kristallographie von $K_2TiSi_6O_{15}$-isotyp mit Dalyit $K_2ZrSi_6O_{15}$. Tschermaks Mineralogische und Petrographische Mitteilungen, 31, 69–79.

Ghose, S. and Wan, C. (1978) Zekterite, $NaLiZr Si_6O_{15}$: a silicate with six-tetrahedral-repeat double chains. American Mineralogist, 63, 304–310.

Gunawardane, R.P., Howie, R.A., and Glasser, F.P. (1982) Structure of lithium sodium yttrium silicate $Na_2LiYSi_6O_{15}$. Acta Crystallographica, B38, 1405–1408.

Haile, S.M., Siegrist, T., Laudise, R.A., and Wuensch, B.J. (1991) Synthesis, structure, and ionic conductivity of $K_3NdSi_6O_{15}$. In G.-A. Nazri, D.F. Shriver, R.A. Huggins, and M. Balkanski, Eds., Solid state ionics II, p. 645–650. Materials Research Society Symposium Proceedings 210.

Haile, S.M., Wuensch, B.J., and Laudise, R.A. (1993a) Hydrothermal synthesis of new alkali silicates: II. Sodium neodymium and sodium yttrium phases. Journal of Crystal Growth, 131, 373–386.

Haile, S.M., Wuensch, B.J., Siegrist, T., and Laudise, R.A. (1993b) Hydrothermal synthesis of new alkali silicates: I. Potassium neodymium phases. Journal of Crystal Growth, 131, 352–372.

Haile, S.M., Maier, J., Wuensch, B.J., and Laudise, R.A. (1995) Structure of $Na_3YSi_6O_{15}$—a unique silicate based on discrete Si_6O_{15} units, and a possible fast-ion conductor. Acta Crystallographica, B51, 673–680.

Haile, S.M., Wuensch, B.J., Laudise, R.A., and Maier, J. (1997) The structure of $Na_3NdSi_6O_{15} \cdot 2H_2O$—a layered silicate with paths for possible fast-ion conduction. Acta Crystallographica, B53, 7–17.

Hill, R.J. and Gibbs, G.V. (1979) Variation in d(T-O), d(T ... T) and $\angle$TOT in silica and silicate minerals, phosphates and aluminates. Acta Crystallographica, B35, 25–30.

Johnson, O., Nielsen, K., and Søtofte, I. (1978) The crystal structure of emeleusite, a novel example of a sechser-doppelkette. Zeitschrift für Kristallographie, 147, 297–306.

Karpov, O.G., Podeminskaya, E.A., and Belov, N.V. (1976) Crystal structure of a K, Ce silicate with a three-dimensional anion framework: $K_2CeSi_6O_{15}$. Soviet Physics Crystallography, 22, 382–384.

Karpov, O.G., Pushcharovskii, D.Y., Pobedimskaya, E.A., Burshtein, I.F., and Belov, N.V. (1977) The crystal structure of the rare-earth silicate $NaNdSi_6O_{13}(OH)_2 \cdot n(H_2O)$. Soviet Physics Dokladay, 22, 464–466.

Kashaev, A.A. and Sapozhnikov, A.N. (1978) Crystal structure of armstrongite. Soviet Physics Crystallography, 23, 539–542.

Kudoh, Y. and Takèuchi, Y. (1979) Polytypism of xonotlite: I. Structure of A $\bar{1}$ polytype. Mineralogical Journal Japan, 9, 349–373.

Lazebnik, K.A., Lazebnik, Y.D., and Makhotko, V.F. (1984) Davanite $(K_2TiSi_6O_{15})$—a new alkaline titanosilicate. Zapiski Vsesoyuznogo Mineralogicheskogo Obshchestva, 113, 95–96.

Liebau, F. (1985) Structural chemistry of silicates: structure, bonding, and classification, p. 204–205. Springer-Verlag, Berlin.

Marr, J.M. and Glasser, F.P. (1979) Synthesis and properties of zekterite, $LiNaZrSi_6O_{15}$, and its isotypes. Mineralogical Magazine, 43, 171–173.

Merlino, S. (1969) Tuhualite crystal structure. Science, 166, 1399–1401.

Nuamova, I.S., Podeminskaya, E.A., Pushcharovskii, D.Y., Belov, N.V., and Altukhova, N.Y. (1976) Crystal structure of a synthetic K-berylosilicate of the epididymite group. Soviet Physics Dokladay, 21, 422–424.

Ohashi, Y. and Finger, L.W. (1978) The role of octahedral cations in pyroxenoid crystal chemistry: I. Bustamite, wollastonite, and the pectolite-schizolite-serandite series. American Mineralogist, 63, 274–288.

Pushcharovskii, D.Y., Karpov, O.G., Pobedimskaya, E.A., and Belov, N.V. (1977) The crystal structure of $K_3NdSi_6O_{15}$. Soviet Physics Dokladay, 2, 292–293.

Quintana, P. and West, A. (1981) Synthesis of $Li_2ZrSi_6O_{15}$, a zekterite-related phase. Mineralogical Magazine, 44, 361–362.

Robinson, P.D. and Fang, J.H. (1970) The crystal structure of epididymite. American Mineralogist, 55, 1541–1549.

Shumyatskaya, N.G., Voronkov, A.A., and Pyatenko, Y.A. (1980) Sazhinite, $Na_2Ce[Si_6O_{14}(OH)] \cdot nH_2O$: a new representative of the dalyite family in crystal chemistry. Soviet Physics Crystallography, 25, 419–423.